Neuroradiology (2013) 55:845–851
DOI 10.1007/s00234-013-1183-4

DIAGNOSTIC NEURORADIOLOGY

MRI of intracranial vertebral artery dissection: evaluation of intramural haematoma using a black blood, variable-flip-angle 3D turbo spin-echo sequence

Koichi Takano · Shinnichi Yamashita · Koichiro Takemoto · Tooru Inoue · Yasuo Kuwabara · Kengo Yoshimitsu

Received: 15 January 2013 / Accepted: 27 March 2013 / Published online: 26 April 2013

Abstract
Introduction We investigated the efficacy of three-dimensional black blood T1-weighted imaging (3D-BB-T1WI) using a variable refocusing flip angle turbo spin-echo sequence in the diagnosis of intracranial vertebral artery dissection (VAD).
Methods Sixteen consecutive patients diagnosed with intracranial VAD underwent magnetic resonance imaging that included 3D time-of-flight-MRA, axial spin-echo T1-weighted images (SE-T1WI) and oblique coronal 3D-BB-T1WI sequences. The visualization, morphology and extent of intramural haematomas were assessed and compared among the sequences. Results obtained by digital subtraction angiography (DSA), 3D-angiography and/or 3D-CT angiography (CTA) were used as standards of reference.
Results 3D-BB-T1WI revealed intramural haematomas in all cases, whereas SE-T1WI and magnetic resonance angiography (MRA) failed to reveal a haematoma in one case and three cases, respectively. The mean visualization grading score for the intramural haematoma was the highest for 3D-BB-T1WI, and there was a statistically significant difference among the sequences ($p<0.001$). At least a portion of the intramural haematoma was distinguishable from the lumen on 3D-BB-T1WI, whereas the haematomas were entirely indistinguishable from intraluminal signals on MRA in two cases (12.5 %) and on SE-T1WI in one case (6.3 %). 3D-BB-T1WI revealed the characteristic crescent shape of the intramural haematoma in 14 cases (87.5 %), whereas SE-T1WI and MRA revealed a crescent shape in only 7 cases (43.8 %) and 8 cases (50 %), respectively. In a consensus reading, 3D-BB-T1WI was considered the most consistent sequence in representing the extent and morphology of the lesion in 14 cases (87.5 %), compared to DSA and CTA.
Conclusion 3D-BB-T1WI is a promising method to evaluate intramural haematoma in patients with suspected intracranial VAD.

Keywords Vertebral artery dissection · Magnetic resonance imaging · MR angiography · Three dimensional · Black blood

K. Takano (✉) · S. Yamashita · Y. Kuwabara · K. Yoshimitsu
Department of Radiology, Faculty of Medicine,
Fukuoka University, 7-45-1 Nanakuma, Jonan-ku,
Fukuoka-shi, Fukuoka 814-0180, Japan
e-mail: k-takano@fukuoka-u.ac.jp

K. Takemoto · T. Inoue
Department of Neurosurgery, Faculty of Medicine,
Fukuoka University, Fukuoka, Japan

Introduction

Dissection of the craniocervical arteries, once considered a rare disease, has become increasingly recognized as a cause of stroke and headache in young and middle-aged individuals. The increasing number of patients in recent years reflects both a growing familiarity with this clinical entity and a significant improvement in neurovascular imaging [1–5].

Selective digital subtraction angiography (DSA) has long been the gold standard for diagnosis and follow-up of arterial dissections. However, this technique does not always ensure definitive diagnosis of dissection because it does not allow visualization of the configuration of the arterial wall and intramural haematoma [2, 3]. In addition, selective DSA can cause complications, including several neurological deficits and iatrogenic dissections [4, 5].

In contrast, magnetic resonance imaging (MRI), magnetic resonance angiography (MRA) and CT angiography (CTA) offer potential advantages for the non-invasive assessment of vascular diseases and have proven useful for the

detection of arterial dissections. Several reports have indicated that the increased use of these non-invasive imaging studies has allowed a greater rate of diagnosis than that determined solely by DSA [1–3, 6–13].

Typically, magnetic resonance (MR) techniques for the evaluation of arterial dissection in the reported studies include routine T1-weighted imaging (T1WI), T2-weighted imaging usually with spatial presaturation, either with or without fat suppression, and MRA with or without gadolinium enhancement. In particular, time-of-flight (TOF) MRA and T1WI can provide direct visualization of subacute intramural haematoma as a high-signal structure due to its short T1 feature [1–3, 6–10].

However, it may be problematic to differentiate between intraluminal flow and intramural haematoma solely on the basis of TOF-MRA. In MRA, intraluminal signal depends on flow velocity, presence of laminar flow and/or turbulence. Therefore, discrimination and detection of intramural haematoma is often difficult [8, 13, 14]. On the other hand, conventional two-dimensional (2D) cross-sectional images are subject to the partial volume effect, and low spatial resolution in the slice-selecting direction may obscure small haematomas. MRI and MRA have been reported to be substantially less sensitive and specific in the diagnosis of vertebral artery dissection (VAD) in comparison with dissection in the internal carotid artery, due to the smaller diameter of the vertebral arteries (VAs), and inability of the techniques to reveal intramural haematoma [6, 8, 15].

For the last decade, a variation of the black blood three-dimensional (3D) turbo spin-echo (TSE) technique, which uses a non-selective variable refocusing flip angle (VRFA) along the echo train to achieve a pseudo-steady state for a low refocusing flip angle, has been introduced. With this technique, a longer echo train can be applied while reducing the specific absorption ratio, image blurring and image contrast degradation [16, 17]. In addition, 3D-VRFA-TSE, combined with a lower refocusing flip angle and a flow-sensitizing gradient, has been reported to efficiently reduce intravascular signals and provide single-slab 3D black blood imaging without the need for cardiac/pulse triggering [18]. Unlike ordinary flow compensation, sensitized flow compensation has an effect of reducing the signal of flowing blood.

A recent study revealed that the 3D-VRFA-TSE technique was useful in detecting vulnerable and soft carotid plaques. The 3D-VRFA-TSE was comparable to gated 2D TSE technique in suppressing intraluminal signals, and superior to 2D-TSE in spatial resolution, showing more morphological details of the plaques [19]. Therefore, it is expected that the 3D-VRFA-TSE sequence, which is capable of achieving three-dimensional black blood T1-weighted imaging (3D-BB-T1WI), may be useful in the detection and assessment of intramural haematomas resulting from arterial dissections.

The purpose of this study was to evaluate the diagnostic capability of 3D-BB-T1WI in assessing intracranial VADs.

Methods

Study population

Our institutional review board approved this study and waived the process of obtaining informed consent because of its retrospective nature. All consecutive patients diagnosed with intracranial VAD between May 2009 and November 2012 were included in this study, if they satisfied the following criteria: (1) compatible clinical picture including headache and/or ischemic symptoms, (2) an initial MR examination within 30 days after the onset of symptoms and (3) unequivocal imaging findings including (a) intimal flap/double lumen/intramural pooling, or (b) the pearl and string sign on CTA and/or DSA [2, 3], or (c) enlargement of the outer diameter of the affected vessel and/or hyperdense intramural haematoma at the site of a steno-occlusive lesion (either stenosis or occlusion) on CTA [11–13]. Patients with imaging findings that indicated moderate to severe atherosclerotic changes were excluded.

A total of 17 patients were enrolled according to the above criteria. One patient was excluded due to the presence of motion artefacts in MRI; thus, a total of 16 patients (12 males and 4 females; age range, 39–64 years; mean age, 50.3 years) were included in the final analysis.

Imaging protocol

MR imaging

All MR imaging procedures were performed using a 1.5-T Philips Achieva whole-body scanner (Philips Medical Systems, Best, the Netherlands) and a SENSE head coil with eight elements.

The standard MR imaging protocol included axial spin-echo (SE) T1WI with a caudal spatial presaturation (repetition time (TR)/echo time (TE), 512–568/12–15; field of view (FOV), 24 cm; 256×204 matrix; 4.5- to 6-mm-thick 20 slices; interslice gap, 0 to 1 mm; NSA, 1 to 2; acquisition time, 1 min 58 s to 3 min 33 s) and 3D TOF-MRA (TR/TE/flip angle, 25/6.9/20; FOV, 15 cm; 302×182 matrix; 120 to 140 slices, 0.6 to 0.65 mm thick; acquisition time, 4 min 32 s to 5 min 22 s). Fat suppression was not applied to either SE-T1WI or MRA.

The 3D-BB-T1WI (TR/TE/echo train length/number of excitations, 450/19/20/2) was obtained in an oblique coronal direction to include the entire third and fourth segments of the VA and the basilar artery. Other parameters included a matrix size of 225×224 with a reconstruction matrix of 512×512, a 15-cm FOV and a refocus flip angle (refocus control) of 60°. A

flow-sensitizing gradient (sensitized flow compensation) was employed to suppress the signal from slowly flowing blood [18, 19]. The acquired section thickness and reconstructed section thickness were 1.0 and 0.5 mm, respectively. In the early course of the study, a parallel imaging technique was not applied, and 50 to 60 slices were acquired in 4 min 17 s to 5 min 8 s. In the later stage of the study, a sensitivity encoding (SENSE) technique was used with a reduction factor of 2.0–100 slices which were acquired in 5 min and 20 s. In most instances (13/16 cases), a chemical shift selective fat suppression of spectral presaturation with inversion recovery (SPIR) was applied to the 3D-BB-T1WI.

MR studies within 30 days after onset were reviewed, and if MR examinations were repeated within the period, the examination that included SE-T1WI that revealed the intramural haematoma most conspicuously was chosen in the consensus reading to be included in the final analysis.

CTA

All 16 patients underwent CTA performed on a 64-detector scanner (Aquilion, Toshiba, Tokyo, Japan) with the following parameters: 1.2 mL/kg of iodinated contrast agent (iopamidol, Iopamiron 370, Bayer Healthcare, Osaka, Japan) up to a maximum of 100 mL, 4 mL/s injection rate, 120 kV, 300 mA, 0.5–0.75 s/rotation, 0.5-mm-thick sections and table speed of 20.5 mm/rotation.

DSA

All 16 patients underwent conventional selective DSA of the VA. In the early stage of the study (four cases), DSA was acquired on an Integris Allura (Philips Healthcare, Best, the Netherlands). In the later stage of this study (12 cases), DSA was acquired on an Artis Zee biplane (Siemens, Erlangen, Germany). In 10 cases, in addition to conventional 2D-DSA, 3D rotational angiography of the lesion was also performed. In seven cases, CT-like reconstructions were created from the 3D dataset on a DynaCT workstation.

Image analysis

Two experienced neuroradiologists blinded to the CTA/DSA findings independently reviewed the 3D-BB-T1WI, SE-T1WI and MRA images and rated the visualization of intramural haematoma using a five-point grading scale: 5=definite (higher signal compared to the adjacent brain), 4=definite, but partially indistinguishable from the lumen or surrounding structure, 3=present, but roughly isointense to the brain, 2=suspected, but difficult to determine (entirely indistinguishable from the lumen or surrounding tissue) and 1=none. Each observer had an interval of at least 2 weeks between reviewing the three imaging sequences, with the order of the cases randomized. Subsequently, any disagreement was resolved by consensus. A qualitative comparison was made using the grades as indices. For the presence of intramural haematoma, grades 3, 4 and 5 were considered positive. The morphology of the haematoma, particularly its characteristic crescent shape on the short-axis view, was also recorded for each MR imaging sequence.

The 3D datasets of MR images (i.e. 3D-BB-T1WI and MRA) were analysed on an image processing software (Aquarius Net, Ver. 1.6.6.1; TeraRecon, San Mateo, CA, USA), and 2D datasets (i.e. SE-T1WI) were analysed on a PACS system (Rapideye Toshiba Medical, Tokyo, Japan).

DSA and CTA findings were reviewed by two senior radiologists, who were unaware of the results from the MRI. The presence of an intimal flap, double lumen, intramural pooling, the pearl and string sign and stenoocclusive change was recorded. Enlargement of the outer diameter of the affected vessel and hyperdense areas indicating intramural haematoma were also recorded on CTA.

Finally, each MRI sequence was compared with DSA and CTA regarding the extent and morphology of the lesion, and the MRI sequence that was most consistent with DSA/CTA among the three sequences was determined at the consensus reading.

Statistical analysis

The interobserver agreement was assessed by calculating the kappa value with a 95 % CI. The Friedman test was used to compare the visualization grading score of intramural haematoma for each MR imaging sequence. If the Friedman test resulted in a p value that indicated a significant difference (<0.05), each pair was tested individually with the Wilcoxon's signed rank test. The detection rate of haematoma (i.e. grades 3, 4 and 5) as well as the presence of the characteristic crescent shape of the haematoma in each sequence was compared using the Cochran Q test followed by a post hoc McNemar test. A p value of <0.0167 (i.e. 0.05/3) was considered significant after Bonferroni correction. Statistical analyses were performed using SPSS software (version 11.0.1, SPSS, Chicago, IL) or spreadsheet software (Excel 2007, Microsoft, Redmond, WA).

Results

Final diagnosis, CTA and DSA

In 12 cases, the diagnosis was made by DSA, which revealed an intimal flap, double lumen, intramural pooling and/or the pearl and string sign. In the remaining four cases, the diagnosis was made on the basis of the visualization of intramural

haematomas at the steno-occlusive lesion on CTA. Both CTA and DSA showed complete occlusion of the affected VA in four patients. CTA showed an enlargement of the outer diameter of the affected vessel and hyperdense material indicating intramural haematoma in 10 cases, including four cases showing total occlusion of the VA.

MRI

MRI studies were obtained 9 to 26 days after the onset of symptoms (mean 16 days). The interobserver agreement for the visualization grading score of intramural haematoma as calculated by the kappa value was 0.58 (95 % CI, 0.18–0.98) for 3D-BB-T1WI, 0.49 (95 % CI, 0.16–0.65) for SE-T1WI and 0.5 (95 % CI, 0.16–0.84) for MRA, respectively.

The 3D-BB-T1WI detected iso- to high-signal intramural haematoma (i.e. grades 3 to 5) in all 16 cases, whereas SE-T1WI and MRA revealed definite haematoma in 15 cases (93.8 %) and 13 cases (87.5 %), respectively. There was no statistically significant difference in the detection rate of haematoma among the sequences (p=0.26).

The visualization grading scores of intramural haematoma in the three MR sequences are summarized in Table 1. On average, the scores on 3D-BB-T1WI were the highest, and there was a statistically significant difference among the sequences (p<0.001). The score for 3D-BB-T1WI was significantly higher than that of MRA (p=0.002). The score was also higher than that for SE-T1WI, but the difference was not significant (p=0.034).

The intramural haematomas were entirely indistinguishable from intraluminal signals (i.e. grade 2) on MRA in two cases (12.5 %) and on SE-T1WI in one case (6.3 %). In contrast, at least a portion of the haematoma was distinguishable from the lumen on 3D-BB-T1WI in all cases.

Table 1 Visualization grading scores of intramural haematoma for each imaging sequence

	Grading score (n = 16)	
3D-BB-T1WI	4.56 (0.63)	*
SE-T1WI	4.31 (0.87)	
MRA	3.81 (0.75)	

Data are mean values (standard deviations)

* p<0.001 in comparing grading scores between imaging sequences

Both 3D-BB-T1WI and MRA allowed visualization of the VA of interest in arbitrary orientations, including oblique short-axis and long-axis views. As a result, 3D-BB-T1WI revealed the characteristic crescent shape of an intramural haematoma in 14 cases (87.5 %), whereas SE-T1WI and MRA revealed a crescent configuration in 7 cases (43.8 %, p<0.0167) and 8 cases (50 %, p=0.031), respectively (Fig. 1).

In the consensus reading, 3D-BB-T1WI was considered most consistent in comparison with DSA and CTA with regard to the extent and morphology of the lesions in 14 cases (87.5 %). In the remaining two cases (12.5 %), 3D-BB-T1WI and MRA were considered equivalent.

On SE-T1WI, a high-signal area was observed within or along the vertebrobasilar artery without abnormality on DSA/CTA in six cases (eight sites), which was considered a false-positive finding. No such finding was noted on 3D-BB-T1WI in any of the cases (Fig. 2).

Discussion

This study investigated the efficacy of 3D-BB-T1WI for assessing intramural haematomas in intracranial VADs. Visualization grading scores of the intramural haematomas on 3D-BB-T1WI were highest among the different sequences, and were significantly higher than those of MRA, although no statistically significant difference was observed for the haematoma detection rate. Unlike SE-T1WI, 3D-BB-T1WI has a higher craniocaudal spatial resolution (0.67 mm) and allows visualization of the VAs in arbitrary orientations. The capability to create obliquely reformatted images enabled visualization of short-axis images of the VAs and the characteristic crescent shape of an intramural haematoma in 14 cases (Fig. 1). In contrast, SE-T1WI is subject to the partial volume effect due to lower craniocaudal resolution (4.5–6mm); therefore, it can be difficult to assess small haematomas using this conventional 2D technique. SE-T1WI could reveal the typical crescent shape of the haematoma in only seven cases.

The MRA used in this study also had a high craniocaudal spatial resolution of 0.6 to 0.65 mm. However, intramural haematomas were entirely indistinguishable from the intraluminal signal in two cases and partially indistinguishable in 13 cases on MRA (Fig. 1). Consequently, the morphology of the haematomas tended to be difficult to evaluate on MRA.

Overall, 3D-BB-T1WI yielded better distinction of intramural haematomas compared to other sequences. Furthermore, iso- to high signal was observed on SE-T1WI in arteries that appeared normal on CTA/DSA in six cases (Fig. 2). These findings were considered flow artefacts because such signals were not noted on 3D-BB-T1WI in any of the cases. These results indicate that spatial presaturation

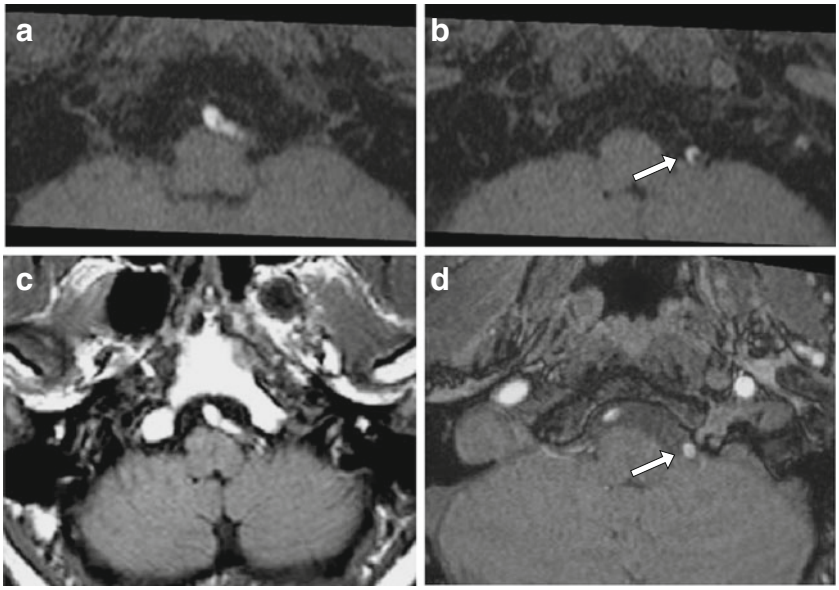

Fig. 1 Case 4. A 41-year-old man with sudden occipital headache. MRI was obtained 20 days after onset. In serial axial reformatted images of 3D-BB-T1WI (**a**, **b**), a high-intensity intramural haematoma of the left VA is clearly shown on both slices. In the caudal slice (**b**), the haematoma exhibits a characteristic crescent shape (*arrow*). In SE-T1WI (**c**), a high-signal haematoma is shown in the left VA. In MRA (**d**), the intramural haematoma is indistinguishable from the lumen (*arrow*)

alone may be insufficient to completely suppress the signal from inflowing blood on SE-T1WI. In 3D-BB-T1WI, suppression of the intravascular signal due to a lower refocusing flip angle and flow-sensitizing gradients (sensitized flow compensation) [13, 14] was helpful in better distinguishing haematomas than either SE-T1WI or MRA.

An imaging approach similar to our 3D-BB-T1WI was reported by Kirsch et al. They employed a spatial presaturation pulse to the caudal side of a TOF-MRA slab (black blood MRA) and achieved 100 % sensitivity and 100 % specificity in detecting intramural haematomas in carotid artery dissections [15]. Although we have not directly compared 3D-BB-T1WI and MRA with presaturation, it is expected that these two techniques attain similarly high levels of sensitivity in detecting intramural haematomas.

There are several limitations in our study. One is the lack of uniformity in the pulse sequences used. In particular, the SE-T1WI imaging protocol varied and fat suppression was not applied. Lack of fat suppression might influence the visualization of a haematoma in the third segment of the VA, which is surrounded by fat [2, 6, 10, 14]. In addition, the field of view of the 3D-BB-T1WI used in this study was limited to the intracranial vertebrobasilar system, third segment (and distal portion of the second segment) of the VA. Since VAD may occur proximal to the area imaged by the 3D-BB-T1WI used in our study, further investigations comparing a 3D-BB-T1WI with a larger FOV and fat-suppressed SE-T1WI would be required to determine the usefulness of 3D-BB-T1WI in the diagnosis of VAD. However, we believe in the validity of the comparison between 3D-BB-T1WI and SE-T1WI without fat

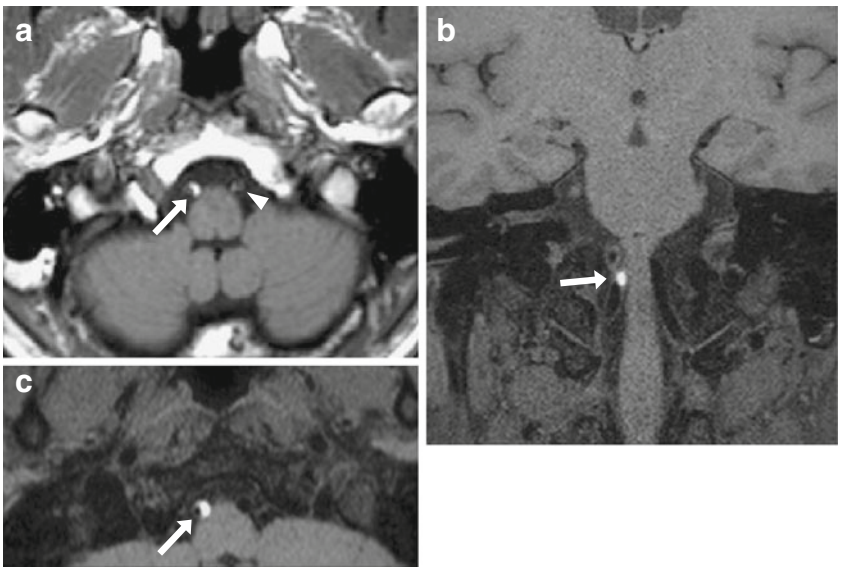

Fig. 2 Case 12. A 47-year-old man with sudden headache. MRI was obtained 9 days after onset. SE-T1WI (**a**) shows a high-intensity intramural haematoma of the right VA (*arrow*). Iso- to high signal is also observed in the left VA (*arrowhead*), which appeared normal on DSA and CTA. 3D-BB-T1WI (**b**) demonstrates the relationship between the intramural hematoma and the lumen. An axial reformatted 3D-BB-T1WI (**c**) shows the characteristic crescent shape of a haematoma (*arrow*). In 3D-BB-T1WI, the high-signal area is not noted in the left VA

suppression to detect dissection of the fourth segment, which is surrounded by low-signal CSF. In East Asian populations, VAD is much more frequently intracranial than extracranial, unlike in Western countries [20, 21]. On the basis of this epidemiological background, we have not applied fat suppression to SE-T1WI in most cases suspected of VAD. In contrast, 3D-BB-T1WI typically includes the distal portion of the second segment and the entire third segment. We applied fat suppression to 3D-BB-T1WI in most cases, since these segments of the VAs are surrounded by fat tissue.

A second limitation is that our study does not include acute stage VAD (i.e. within 7 days of onset). We chose the examination that included SE-T1WI that revealed the intramural haematoma most conspicuously in the consensus reading, to make it easy to compare the visualization of the haematomas among the sequences. Two cases (case 2 and case 8) underwent their first MRI on the day after onset and an isointense haematoma was observed in each, although the morphology of the haematoma was more easily defined on 3D-BB-T1WI.

A third limitation is that we did not conduct a case–control study, and therefore, the specificity of each imaging sequence could not be determined. There are various phenomena that can mimic intramural haematomas, such as turbulent or stagnant intravascular flow and flow artefacts from CSF. In a preliminary study of BB-T1WI sequences, we found that the flow of CSF resulted in flow void, rather than high-signal inflow artefacts on 3D-BB-T1WI. In a few instances, intra-arterial flow was not completely suppressed, although we have not noted an intraluminal signal that is higher than that of the adjacent brain in the control subjects (unpublished data). In the present study, 3D-BB-T1WI did not show iso- to high-signal false positives at normal-appearing arteries in any cases, unlike SE-T1WI. Thus, it is expected that 3D-BB-T1WI has better specificity than SE-T1WI.

Another possible condition identified in the differential diagnosis of intramural haematoma is atherosclerotic plaque. High-signal intensity in carotid plaques on T1-contrast MRI has been widely considered to correspond to soft plaques, which correlate to a higher level of ischemic events. Recently, Turan et al. reported the use of high-resolution black blood T1WI on a 3-T MRI to detect high-intensity plaque of the middle cerebral arteries [22]. Similarly, it is possible that some atherosclerotic plaques of the VAs may show high-signal intensity on T1-contrast MRI. In our study, we have adopted diagnostic criteria attempting to exclude atherosclerosis in the study population. Although it is possible that the evaluation of the outer diameter of the affected vessels [6, 15] and of temporal changes [8, 23] may help in distinguishing atherosclerotic plaques from VADs, further studies are required to investigate whether it is possible to differentiate between these two entities.

Conclusions

3D-BB-T1WI can improve the assessment of intramural haematomas in VAD, compared to SE-T1WI and TOF-MRA. Further studies will be required to establish its true specificity and diagnostic accuracy, as well as its usefulness in assessing extracranial artery dissections, and differentiating VAD from atherosclerotic plaque.

Conflict of interest We declare that we have no conflict of interest.

References

1. Provenzale JM, Sarikaya B (2009) Comparison of test performance characteristics of MRI, MR angiography, and CT angiography in the diagnosis of carotid and vertebral artery dissection: a review of the medical literature. Am J Roentgenol 193:1167–1174
2. Rodallec MH, Marteau V, Gerber S et al (2008) Craniocervical arterial dissection: spectrum of imaging findings and differential diagnosis. Radiographics 28:1711–1728
3. Debette S, Leys D (2009) Cervical-artery dissections: predisposing factors, diagnosis, and outcome. Lancet Neurol 8:668–678
4. Willinsky R, Taylor S, TerBrugge K et al (2003) Neurologic complications of cerebral angiography: prospective analysis of 2,899 procedures and review of the literature. Radiology 227:522–528
5. Kaufmann TJ, Huston J 3rd, Mandrekar JN et al (2007) Complications of diagnostic cerebral angiography: evaluation of 19,826 consecutive patients. Radiology 243:812–819
6. Lévy C, Laissy JP, Raveau V et al (1994) Carotid and vertebral artery dissections: three-dimensional time-of-flight MR angiography and MR imaging versus conventional angiography. Radiology 190:97–103
7. Kitanaka C, Tanaka J, Kuwahara M et al (1994) Magnetic resonance imaging study of intracranial vertebrobasilar artery dissections. Stroke 25:571–575
8. Mascalchi M, Bianchi MC, Mangiafico S et al (1997) MRI and MR angiography of vertebral artery dissection. Neuroradiology 39:329–340
9. Auer A, Felber S, Schmidauer C et al (1998) Magnetic resonance angiographic and clinical features of extracranial vertebral artery dissection. J Neurol Neurosurg Psychiatry 64:474–481
10. Leclerc X, Lucas C, Godefroy O et al (1999) Preliminary experience using contrast-enhanced MR angiography to assess vertebral artery structure for the follow-up of suspected dissection. Am J Neuroradiol 20:1482–1490
11. Chen CJ, Tseng YC, Lee TH et al (2004) Multisection CT angiography compared with catheter angiography in diagnosing vertebral artery dissection. Am J Neuroradiol 25:769–774
12. Vertinsky AT, Schwartz NE, Fischbein NJ et al (2008) Comparison of multidetector CT angiography and MR imaging of cervical artery dissection. Am J Neuroradiol 29:1753–1760
13. Elijovich L, Kazmi K, Gauvrit JY et al (2006) The emerging role of multidetector row CT angiography in the diagnosis of cervical arterial dissection: preliminary study. Neuroradiology 48:606–612
14. Provenzale JM, Sarikaya B, Hacein-Bey L et al (2011) Causes of misinterpretation of cross-sectional imaging studies

for dissection of the craniocervical arteries. Am J Roentgenol 196:45–52
15. Kirsch E, Kaim A, Engelter S et al (1998) MR angiography in internal carotid artery dissection: improvement of diagnosis by selective demonstration of the intramural haematoma. Neuroradiology 40:704–709
16. Hennig J, Weigel M, Scheffler K (2003) Multiecho sequences with variable refocusing flip angles: optimization of signal behavior using smooth transitions between pseudo steady states (TRAPS). Magn Reson Med 49:527–535
17. Busse RF, Hariharan H, Vu A, Brittain JH (2006) Fast spin echo sequences with very long echo trains: design of variable refocusing flip angle schedules and generation of clinical T2 contrast. Magn Reson Med 55:1030–1037
18. Park J, Kim EY (2010) Contrast-enhanced, three-dimensional, whole-brain, black-blood imaging: application to small brain metastases. Magn Reson Med 63:553–561
19. Takano K, Yamashita S, Takemoto K et al (2012) Characterization of carotid atherosclerosis with black-blood carotid plaque imaging using variable flip-angle 3D turbo spin-echo: comparison with 2D turbo spin-echo sequences. Eur J Radiol 81:e304–e309
20. Tsukahara T, Minematsu K (2010) Overview of spontaneous cervicocephalic arterial dissection in Japan. Acta Neurochir Suppl 107:35–40
21. Kim BM, Kim SH, Kim DI et al (2011) Outcomes and prognostic factors of intracranial unruptured vertebrobasilar artery dissection. Neurology 76:1735–1741
22. Turan TN, Bonilha L, Morgan PS et al (2011) Intraplaque hemorrhage in symptomatic intracranial atherosclerotic disease. J Neuroimaging 21:e159–e161
23. Yoshimoto Y, Wakai S (1997) Unruptured intracranial vertebral artery dissection. Clinical course and serial radiographic imagings. Stroke 282:370–374